

Two Information Entropies of Square-Lattice $\pm J$ Ising Models

Xiao Xu (徐晓), Zhongquan Mao (毛忠泉), Xi Chen (陈熹)*

Department of Physics, South China University of Technology, Guangzhou 510640,
China

Abstract: Two information entropies, S_{IB} based on the local bonding energy configurations and S_{IS} based on the local spin configurations, are applied in the square-lattice $\pm J$ Ising systems with Monte Carlo simulations. With S_{IB} and S_{IS} , the spin glass states can be distinguished from paramagnetic states clearly. The results reveal that the nature of spin glass states is of ordering in bonding energy and disordering in spin orientations. The consistence of S_{IB} and the thermodynamic entropy is found.

Keywords: spin glass, entropy, information entropy, phase transition.

PACS: 75.10.Nr, 64.60.Cn, 65.40.gd

* xichen@scut.edu.cn

Spin glass (SG), though has been studied for decades as a prototype of the systems with frustration and disorder[1,2,3], still puzzles us: its spin configuration keeps disordered at low temperature while the diminishment of its entropy occurs [1], indicating SG is an ordered state. According to Landau's theory, the correlation length [4,5] is a unified order parameter for an order-to-disorder phase transition. In SG, however, the correlation length is hard to calculate due to the disordered spin configuration [6]. Therefore Edwards and Anderson had introduced an order parameter q_{EA} for SG. [7,8,9] However this order parameter vanishes in some systems when the system size and the observation time trend to infinite. [3,10,11] Experimentally, the cusp of the AC magnetic susceptibility [12,13], which could be deduced from q_{EA} theoretically [7], and the maximum of heat capacity [14] are used to identify the critical temperature T_c of the SG transition. However, the peak position of the AC magnetic susceptibility shifts to higher T_c with the frequency increasing [15]; and the maximum of heat capacity [7], derived from Ehrenfest's phase classifications, does not correspond to T_c for the problem of so-called 'configurational entropy' in SG [16]. The determination of the spin glass state is still a challenge.

It is well recognized that entropy is the measure of disorder in physics. Hence the thermodynamic entropy could be used to describe the SG disorder. In practice, it is difficult to estimate the Boltzmann-Gibbs (BG) entropy of a large thermodynamic system because of the tremendous number of microstates. [17,18] Fortunately, a kind of *information entropy* can be calculated based on the probability distribution of a certain characteristics for a system. [19,20] It is found that, in ferromagnetic systems,

the information entropies show peaks near T_c . [21,22,23] Moreover, several information entropies have been used to study the order-to-disorder transitions. [24,25] These hint strongly that information entropies corresponding to the features of SG may provide a new sight to the puzzle of disordered spin configurations in ordered state.

According to the information theory, the information entropy can be defined mathematically based on one discrete probability distribution of some feature and represents the disorder of this feature no matter what the feature is. [19,20] In this letter, we defined two information entropies, S_{IB} , based on the local bonding energy configuration, and S_{IS} , on the local spin configuration, respectively in the square-lattice $\pm J$ Ising systems [1,26,27,28] under zero-field conditions and compared them with the thermodynamic entropy S_T . By extensive Monte Carlo (MC) simulations, we found that both ferromagnetic (FM) and antiferromagnetic (AF) states can be distinguished from paramagnetic (PM) phase by either S_{IB} or S_{IS} , but only S_{IB} can be used to differentiate SG state from PM phase. Furthermore, we demonstrate that S_{IB} is almost linear with S_T . The consistence of S_{IB} and S_T suggests that the order of SG is from the ordered bonding energy configurations.

Consisting of a central spin, four nearest spins and four bonds between them, a basic cell (BC) is chosen to estimate the information entropies for a square-lattice $\pm J$ Ising system with $N \times N$ Ising spins from local zones. According to the spin configurations, there are $2^5 = 32$ states with ‘up’ or ‘down’ directions for each spin, while according to the bonding energy configuration, there are $2^4 = 16$ states with ‘high’ or ‘low’

energy state for each bond. Under the periodic boundary condition, $N \times N$ BCs can be extracted.

For a local spin configuration state i , the probability of finding this state, $p_{S,i}$, is

$$p_{S,i} = \frac{N_{S,i}}{N_{\Sigma}} \quad (1)$$

where $N_{S,i}$ is the number of BCs on State i of spin configurations extracted from the system and N_{Σ} is the total number of BCs, i.e. $N_{\Sigma} = N \times N$. Then the information entropy of the system on spin configurations is,

$$S_{IS} = - \sum_{i=1}^{n_s} p_{S,i} \ln(p_{S,i}) \quad (2)$$

where $n_s (= 32)$ is the total number of states of the spin configurations. Similarly, the information entropy on bonding energy configurations can be written as

$$S_{IB} = - \sum_{i=1}^{n_B} p_{B,i} \ln(p_{B,i}) \quad (3)$$

where $p_{B,i} = \frac{N_{B,i}}{N_{\Sigma}}$ is the probability of finding State i of bonding energy configurations, $N_{B,i}$ is number of BCs staying on State i of bonding energy configurations in a system, and $n_B (= 16)$ is the total number of states of the bonding energy configurations. From the information theory perspective, S_{IS} represents the disorder of spin configuration of the system since it is calculated from the local spin configurations, and S_{IB} represents the disorder of bonding energy.

On the other hand, according to the thermodynamic cardinal equation, under zero-field condition, with the change in the system's volume ignored, the derivative of thermal entropy S_T per spin to temperature T is

$$\frac{1}{N_\Sigma} \frac{dS_T}{dT} = C/T \quad (4)$$

where C is the heat capacity per spin. Obviously, one can compare C/T with $\frac{dS_{IS}}{dT}$ or $\frac{dS_{IB}}{dT}$ directly to find the relationship between S_T and S_{IS} or S_{IB} .

The Monte Carlo simulations were performed on the square-lattice Ising systems with the nearest-neighbor coupling J_{ij} . Under zero-field condition, the Hamiltonian of the system is,

$$H = - \sum_{\langle ij \rangle} J_{ij} \sigma_i \sigma_j \quad (5)$$

where σ_i is the Ising spin, and the sums $\langle ij \rangle$ runs over all the nearest-neighbor pairs of spins. The interaction energy J_{ij} takes $\pm J$ ($J > 0$) randomly with the probability distribution,

$$P(J_{ij}) = r\delta(J_{ij} + J) + (1-r)\delta(J_{ij} - J) \quad (6)$$

where r is the ratio of the number of AF bonds to that of all the bonds in a system. Here $r = 0$ for a typical FM system, $r = 1$ for a typical AF system and $r = 0.5$ for a standard EA glass model. Then the heat capacity (per spin) is,

$$C = \frac{1}{N_\Sigma} \frac{dH}{dT} \quad (7)$$

All Monte Carlo simulations are performed with a sequential heat-bath algorithm [29,30]. As the spin glass is an non-equilibrium state, the system should always evolve [10], which should affect the stability of S_{IB} and S_{IS} . Hence we check the evolutions of S_{IB} and S_{IS} with $r = 0.5$ at two temperature points near T_c with 1.6×10^6 MC steps. No evolving phenomenon for S_{IB} and S_{IS} could be observed after 3000 MC steps. Thus 10^4 MC steps are employed for thermal equilibrium at each

temperature for all simulations. The temperature T is reduced by J/k_B , where k_B is the Boltzmann constant. To simplify the calculation, we set $J=1$.

The temperature T and dilution ratio r dependence of S_{IS} and S_{IB} are displayed in Fig 1 (a) and (b) respectively with $r = 0, 1/21, 2/21, \dots, 1$. Here the system size is 100×100 spins and the result is averaged over 64 simulations with different initial spin configurations and bond distributions at a high temperature. In both (a) and (b), S_{IB} and S_{IS} decreases rapidly when a system transits into an AF or FM state from the PM states. Only S_{IB} can give the SG states a lower terrace and the PM states a higher one while S_{IS} shows an undivided platform for SG and PM states. Furthermore, S_{IB} is symmetric along $r = 0.5$, while the symmetry of S_{IS} is broken since the two orientations of spins in AF systems appear equally likely but not in FM systems.

As expected, both S_{IS} and S_{IB} are relatively large in PM states since spins are independently disordered of each other. In FM and AF states, the spins are strongly correlated and well aligned. Hence both S_{IS} and S_{IB} are relatively small. Interestingly, in SG states, the values of S_{IS} are close to those in PM states, while the values of S_{IB} are smaller than those in PM states but clearly larger than those in FM and AF states. It is well known that the spins are correlated in SG despite of the disordered spin configurations. Our results clearly demonstrate the nature of energy order in the spin disorders in SG.

$\frac{dS_{IB}}{dT}$, $\frac{dS_{IS}}{dT}$ and C/T are calculated to investigate the relationship between the thermodynamic entropy S_T and the information entropies S_{IB} and S_{IS} . As shown in Fig.2, C/T is almost proportional to $\frac{dS_{IB}}{dT}$ while it is apparently different from $\frac{dS_{IS}}{dT}$,

and hence S_{IB} and S_T behave similarly.

As shown in Ref. 26, the entropy of SG states approaches a non-zero constant when the temperature approaches zero, and at very high temperatures the entropy of PM approaches a higher constant. A dramatic change of entropy occurs between SG and PM states. It makes sense to use the maximum of C/T , i.e. $\frac{1}{N_\Sigma} \frac{dS_T}{dT}$ as shown in Eq. (4), for determining the phase transition temperature T_c .

The precise derivatives of different entropies to temperature for the FM system ($r = 0$) with 400×400 spins and the SG system ($r = 0.5$) with 200×200 spins are displayed in Fig. 3 (a) and (b) respectively. To accelerate the simulations, the sequential Metropolis algorithm [31] instead of the heat-bath algorithm is used to update the spins in the FM system. Here the averages are preformed over 90 simulations for the FM system and 60 simulations for SG system.

For the square-lattice Ising FM magnet ($r = 0$), the analytical solution gives $T_c = 2.2692$. [32,33] By fitting the magnetic moment data with $M = M_0 (1 - T/T_c)^{1/8}$, we obtain $T_c = 2.265 \pm 0.004$, very close to the analytical result. The peaks of $\frac{dS_{IS}}{dT}$, $\frac{dS_{IB}}{dT}$ and C/T are at 2.267 ± 0.005 , 2.268 ± 0.005 and 2.269 ± 0.005 as shown in Fig.3(a). Obviously all these peak positions can not be distinguished from the analytical result in the context of experimental precise. Not surprisingly, the $\frac{dS_{IB}}{dT}$ is almost proportional to the C/T . It should be noticed that the $\frac{dS_{IS}}{dT}$ is sharper than the $\frac{dS_{IB}}{dT}$, since the strong ergodic breaking gives rise to the symmetry breaking of spin orientations in ferromagnetic systems [34].

For the typical EA SG ($r = 0.5$) shown in Fig.3 (b), the C/T and $\frac{dS_{IB}}{dT}$ behave similar, but their peak positions are not coincident with each other: 1.11 ± 0.03 for C/T and 1.24 ± 0.03 for $\frac{dS_{IB}}{dT}$ which are close to the freezing temperature $T_f \approx 1.25$ by EA parameter q_{EA} [26] and the critical temperature $T_c \approx 1.3$ with the replica number equals to 2 [35]. When we enlarge the basic cell to 3×3 spins with 12 bonds connecting neighbor spins, the $\frac{dS_{IB}}{dT}$ vs. T curve shifts more close to C/T curve (not shown in this paper) and the phase transition point $T_c \approx 1.14$. It means by increasing the size of a basic cell, one can reduce the disparity between the information entropy and the thermodynamic entropy. A big cell, however, will bring up a tremendous expansion of the calculation.

Why does S_{IB} , but not S_{IS} , behave similar to the thermal entropy S_T ? The reason is that both S_T and S_{IB} relate to the energy distribution of the system while S_{IS} only relates to the spin configurations. When the spin configurations strongly rely on the energy distribution such as in the FM or AF phase, S_{IS} has similar behavior as S_T . However in SG state, due to the frustrations, the corresponding relationship between spin configurations and energy distributions misses. Hence S_{IS} can not reveal the changes of S_T .

Here we interpret the linear relationship between S_T and S_{IS} as following.

The Hamiltonian of a system can be carried out with,

$$H = \frac{1}{2} N_{\Sigma} \cdot \sum_{i=1}^{n_B} p_{B,i} H_i \quad (8)$$

where H_i is the Hamiltonian of a BC in State i of bonding energy configurations. For the convenience of calculation, set '0' for the energy of the bond staying on the low

level and ‘2’ for that on the high level. Then H_i equals to 2 times of the number of high level bonds exist in a BC of State i .

From Eq. (4), (7) and (8), one has,

$$\frac{dS_T}{dT} = N_\Sigma \cdot \sum_{i=1}^{n_B} \frac{H_i}{2T} \frac{dp_{B,i}}{dT} \quad (9)$$

Considering the information entropy on bonds defined as Eq. (3), one has,

$$\begin{aligned} \frac{dS_{IB}}{dT} &= - \frac{d \left(\sum_{i=1}^{n_B} p_{B,i} \right)}{dT} - \sum_{i=1}^{n_B} \frac{dp_{B,i}}{dT} \ln p_{B,i} \\ &= \sum_{i=1}^{n_B} \frac{dp_{B,i}}{dT} \ln (1/p_{B,i}) \end{aligned} \quad (10)$$

If the $\ln(1/p_{B,i})$ is linear to $\frac{H_i}{2T}$, i.e.

$$\ln(1/p_{B,i}) = a \frac{H_i}{2T} + b(T) \quad (11)$$

where a is the scaling factor and b is the intercept, one has

$$\begin{aligned} \frac{dS_{IB}}{dT} &= a \sum_{i=1}^{n_B} \frac{dp_{B,i}}{dT} \frac{H_i}{2T} + b(T) \sum_{i=1}^{n_B} \left(\frac{dp_{B,i}}{dT} \right) \\ &= a \sum_{i=1}^{n_B} \frac{dp_{B,i}}{dT} \frac{H_i}{2T} + b(T) \frac{d \left(\sum_{i=1}^{n_B} p_{B,i} \right)}{dT} \\ &= a \sum_{i=1}^{n_B} \frac{dp_{B,i}}{dT} \frac{H_i}{2T} \end{aligned} \quad (12)$$

Camparing Eq. (12) with Eq. (9), we have

$$\frac{dS_T}{dT} \propto \frac{dS_{IB}}{dT} \quad (13)$$

If the BCs are independent of each other, the energy of BCs follows Boltzmann distribution, and hence Eq. (13) holds. However this relationship could be changed since the couplings between the BCs can affect the distributions of bonds.

Interestingly our simulations demonstrate $\frac{dS_T}{dT}$ is almost proportional to $\frac{dS_{IB}}{dT}$. This

implies that the couplings between BCs have no remarkable influence on the slopes a given by Eq. (11) near phase transition point where the information entropy varies dramatically. Shown as an example in Fig.4, for $r = 0.5$, the slopes a of fitting lines for the functions $\ln(1/p_{B,i})$ of $H_i/2T$ are about 2.0 near the phase transition point, which means $\frac{dS_T}{dT}$ is proportional to $\frac{dS_{IB}}{dT}$ in the critical zone. The slope a deviates from 2.0 at low temperature, e.g. $a \approx 0.9$ at $T = 0.1$. However $\frac{dS_T}{dT}$ and $\frac{dS_{IB}}{dT}$ approach zero at low temperature, which have weak affection on the linear relationship between S_T and S_{IB} . We checked all systems for $r = 0$ to 1 and found that the slope a maintains a constant near the critical temperature. Interestingly, $\ln(1/p_{B,i})$ has a better linearity with $H_i/2T$ above T_c than that below T_c although the fitting slope a keeps changeless. It seems that a constant slope a at the vicinity of T_c is the key factor for the linearity between S_{IB} and S_T .

Our derivation suggest that if one could find a local energy distribution $p_{B,i}$ with $\ln p_{B,i}$ approximately linear to aH_i/T at the vicinity of T_c , the information entropy S_{IB} , which is linear to the thermodynamic entropy S_T , could be always calculated.

In conclusion, we define the information entropies S_{IS} and S_{IB} based on the local spin configurations and local bonding energy configurations respectively, and apply them to the $\pm J$ systems. We clarify that SG is a state disordered in spin configurations and ordered in bonding energy configurations. It is found that S_{IB} is nearly linear to the thermodynamic entropy when $\ln p_{B,i}$ is approximately linear to aH_i/T at the vicinity of T_c .

Thanks our colleagues, Prof. Jiang Zhang, Prof. Hongjun Quan, Prof. Yujun Zhao, and

Prof. Xiaobao Yang for the discussions. Fruitful discussions with Prof. Zexian Cao in Institute of Physics, Chinese Academy of Sciences, Beijing, are gratefully acknowledged. This work is supported by NSFC Grant Nos. 11174083 and 11304098.

Reference:

- 1 K. Binder and A. P. Young, *Rev. Mod. Phys.* **58**, 801 (1986).
- 2 A. P. Ramirez, *Annu. Rev. Mater. Sci.* **24**, 453 (1994).
- 3 C. M. Newman and D. L. Stein, *J. Phys.: Condens. Matter* **15**, R1319 (2003).
- 4 T. T. Wu, B. M. McCoy, C. A. Tracy, and E. Barouch, *Phys. Rev. B* **13**, 316 (1976).
- 5 D. S. Fisher and D. A. Huse, *Phys. Rev. B* **38**, 386 (1988).
- 6 Y. Han, Y. Shokef, A. M. Alsayed, P. Yunker, T. C. Lubensky, and A. G. Yodh, *Nature* **456**, 898 (2008).
- 7 S. F. Edwards and P. W. Anderson, *J. Phys. F: Metal Phys.* **5**, 965 (1975).
- 8 D. Sherrington and S. Kirkpatrick, *Phys. Rev. Lett.* **35**, 1792 (1975).
- 9 G. S. Grest and E. G. Gabl, *Phys. Rev. Lett.* **43**, 1182 (1979).
- 10 A. J. Bray, M. A. Moore, and P. Reed, *J. Phys. C: Solid State Phys.* **11**, 1187 (1978).
- 11 I. Morgenstern and K. Binder, *Phys. Rev. B* **22**, 288 (1980).
- 12 J. L. Dormann, L. Bessais and D. Fiorani, *J. Phys. C: Solid State Phys.* **21**, 2015 (1988).
- 13 J. Wu and C. Leighton and *Phys. Rev. B* **67**, 174408 (2003),
- 14 L. E. Wenger and P. H. Keesom, *Phys. Rev. B* **13**, 4053 (1976).
- 15 S. Sahoo, PHD dissertation, Interacting magnetic nanoparticles in discontinuous $\text{Co}_{80}\text{Fe}_{20}/\text{Al}_2\text{O}_3$ multilayers and in granular $\text{FeCl}_2\text{-Fe}$ heterostructures, Standort

Duisburg (2003).

- 16 Th. M. Nieuwenhuizen, Phys. Rev. Lett. **79**, 1317 (1997).
- 17 B. A. Berg and T. Celik, Phys. Rev. Lett. **69**, 2292 (1992).
- 18 E. E. Vogel, J. Cartes, S. Contreras, W. Lebrecht, and J. Villegas, Phys. Rev. B **49**, 6018 (1994).
- 19 Th. M. Cover, J. A. Thomas, Elements of Information Theory, 2nd Edition, Char. 2, John Wiley & Sons, Inc., ISBN-13978-0-471-24195-9 (2006).
- 20 Th. M. Cover, J. A. Thomas, Elements of Information Theory, 2nd Edition, Char. 11.10 and Char. 17, John Wiley & Sons Inc., ISBN-13978-0-471-24195-9 (2006). In these chapters, the relationship between Fisher Information, a measurement of probability distribution, and Shannon entropy is discussed. By these discussions, one can get a clear understanding of the relationship between a probability distribution and its Shannon entropy.
- 21 S. Gu, C. Sun, and H. Lin, J. Phys. A: Math. Theor. **41**, 025002 (2008).
- 22 H. Matsuda, K. Kudo, R. Nakamura, O. Yamakawa, and T. Murata, Int. J. Theo. Phys. **35**, 839 (1996).
- 23 L. Barnett, J. T. Lizier, M. Harré, A. K. Seth, and T. Bossomaier, Phys. Rev. Lett. **111**, 177203 (2013).
- 24 T. Vicsek, A. Czirók, E. Ben-Jacob, I. Cohen, and O. Shochet, Phys. Rev. Lett. **75**, 1226 (1995).
- 25 R. T. Wicks, S. C. Chapman, and R. O. Dendy, Phys. Rev. E **75**, 051125 (2007).
- 26 S. Kirkpatrick, Phys. Rev. B **16**, 4630 (1977).
- 27 R. Fisch and A. K. Hartmann, Phys. Rev. B **75**, 174415 (2007).
- 28 O. Melchert and A. K. Hartmann, Phys. Rev. B **79**, 184402 (2009).
- 29 Y. Miyatake, M. Yamamoto, J. J. Kim, M. Toyonaga, and O. Nagai, J. Phys. C:

Solid State Phys. **19**, 2539 (1986).

30 M. Acharyya and D. Stauffer, Eur. Phys. J. B **5**, 571 (1998).

31 G. Bhanot, Rep. Prog. Phys. **51**, 429 (1988).

32 H. A. Kramers and G. H. Wannier, Phys. Rev. **60**, 252 (1941).

33 R. J. Baxter, Exactly Solved Models in Statistical Mechanics, Acad. Press Inc., ISBN 978-0-12-083180-7 (1982).

34 R. G. Palmer, Advances in Phys. **31**, 669 (1982).

35 J. Maillard, K. Nemoto, and H. Nishimori, J. Phys. A: Math. Gen. **36**, 9799 (2003).

Figure Captions:

Figure 1 The contours of (a) S_{IS} and (b) S_{IB} as the functions of r and T . FM, SG, AF and PM states are marked in (b) based on different color zones, while SG and PM can not be distinguished from each other in (a).

Figure 2 The C/T (blue solid lines), dS_{IS}/dT (green dash dot lines) and dS_{IB}/dT (red dash lines) as the functions of T under $r = 2/21$ (a), $5/21$ (b), $9/21$ (c), and $19/21$ (d).

Figure 3 (a) Normalized C/T , $\frac{dS_{IS}}{dT}$ and $\frac{dS_{IB}}{dT}$ for $r = 0$, and (b) C/T and $\frac{dS_{IB}}{dT}$ for $r = 0.5$ as the function of temperatures. In (b), 10000 MC steps are performed for averages after 10000 MC steps for thermal equilibrium at each temperature.

Figure 4 The relationships between $\ln(1/p_{B,i})$ and $H_i/2T$ for $r = 0.5$ at the temperature range between 0.6 and 1.8. There are 1 state for $H_i = 0$, 4 states for $H_i = 2$, 6 states for $H_i = 4$, 4 states for $H_i = 6$, and 1 state for $H_i = 8$ at each temperature point, and for $H_i = 4$, the markers split into two branches, the lower branch for the states with the two high level bonds staying on the symmetric positions about the central spin, and the upper branch for the others. Four lines, labeled as A, B, C and D, are the linear fitting lines for $\ln(1/p_{B,i})$ with different H_i at $T = 1.8$ (■), 1.4 (◆), 1.0 (●) and 0.6 (▲) respectively. The slopes of the fitting lines are 2.0, 2.0, 2.0, and 1.8, respectively. Here all data for $p_{B,i} < e^{-10}$ are ignored due to a large estimation error in the 200×200 systems.

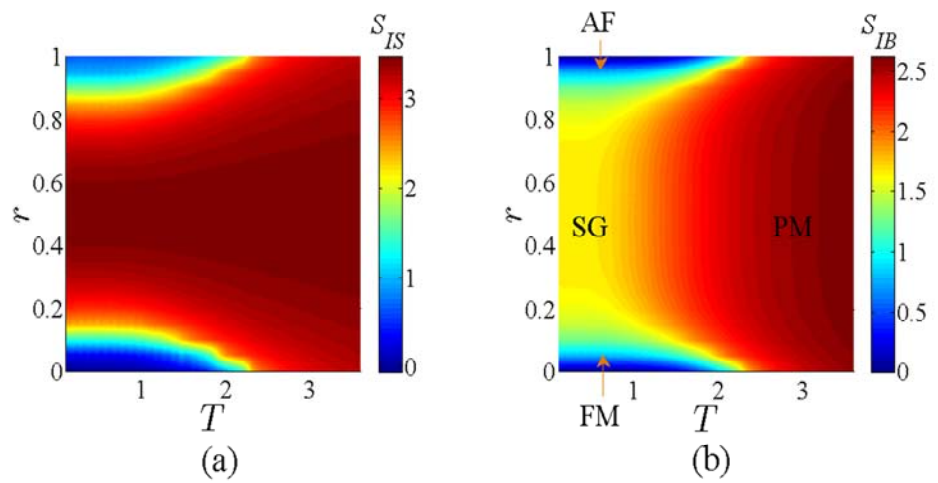


Fig. 1 Xiao Xu et al.

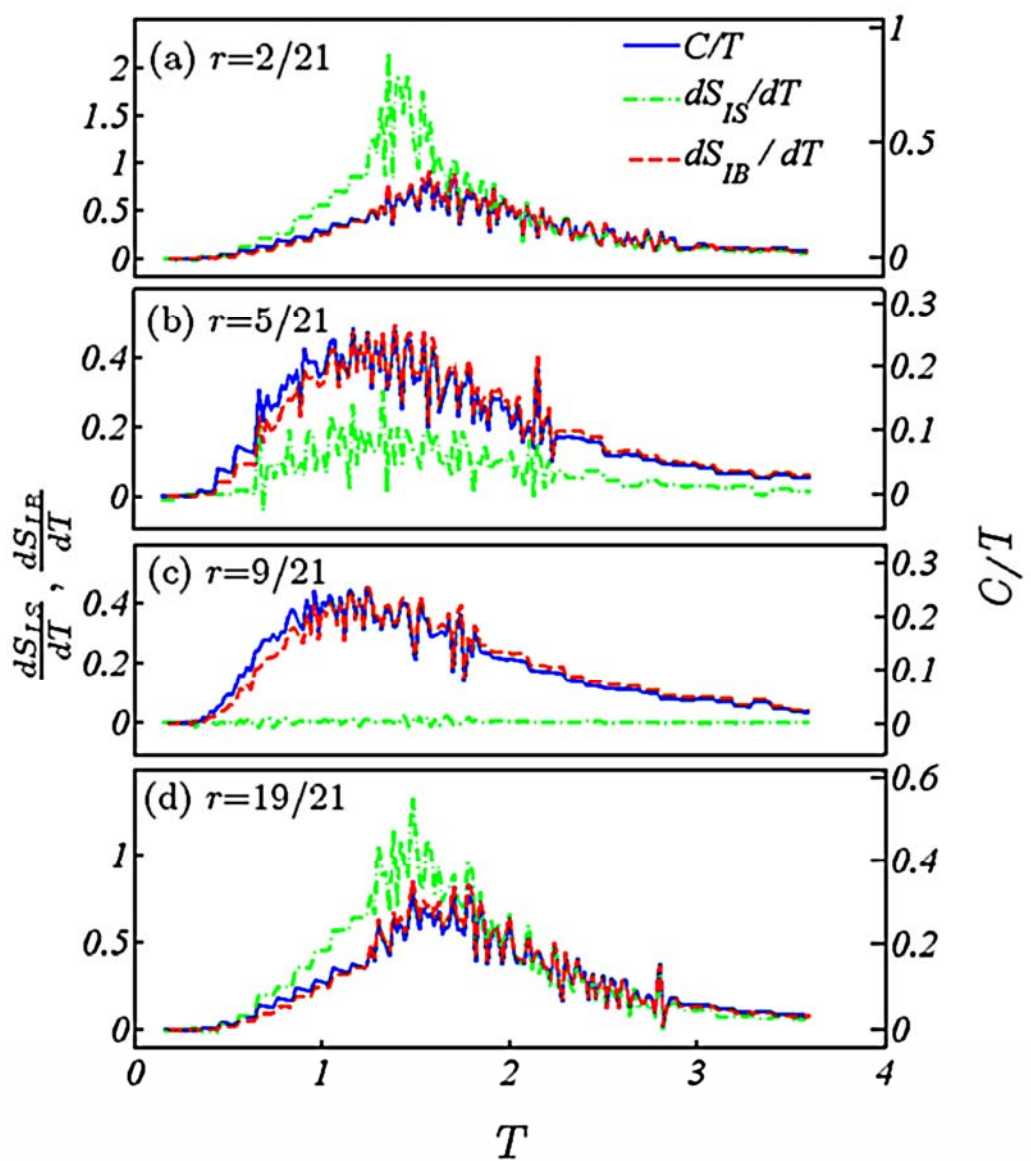


Fig. 2 Xiao Xu et al.

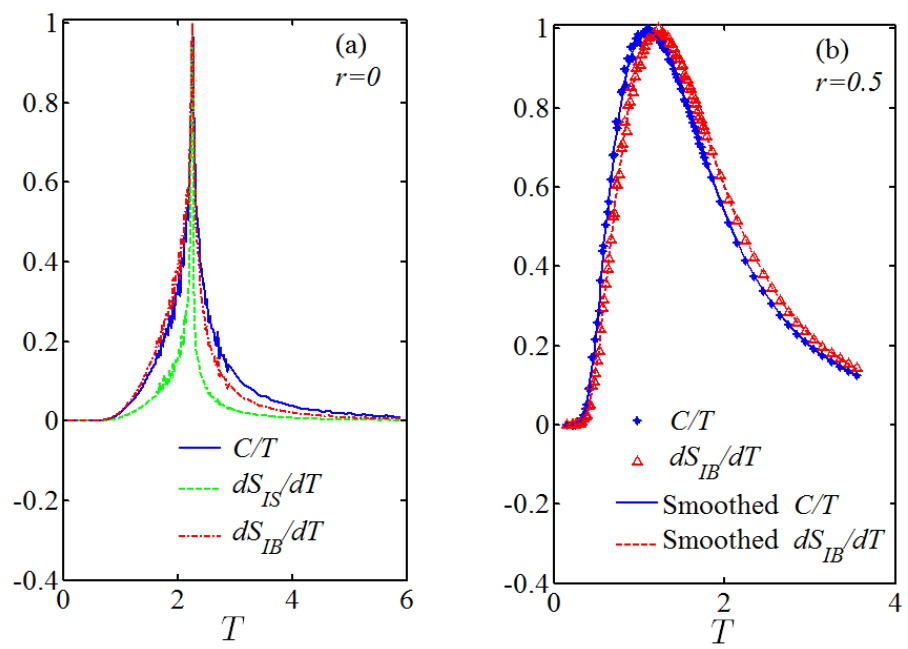


Fig.3 Xiao Xu et al.

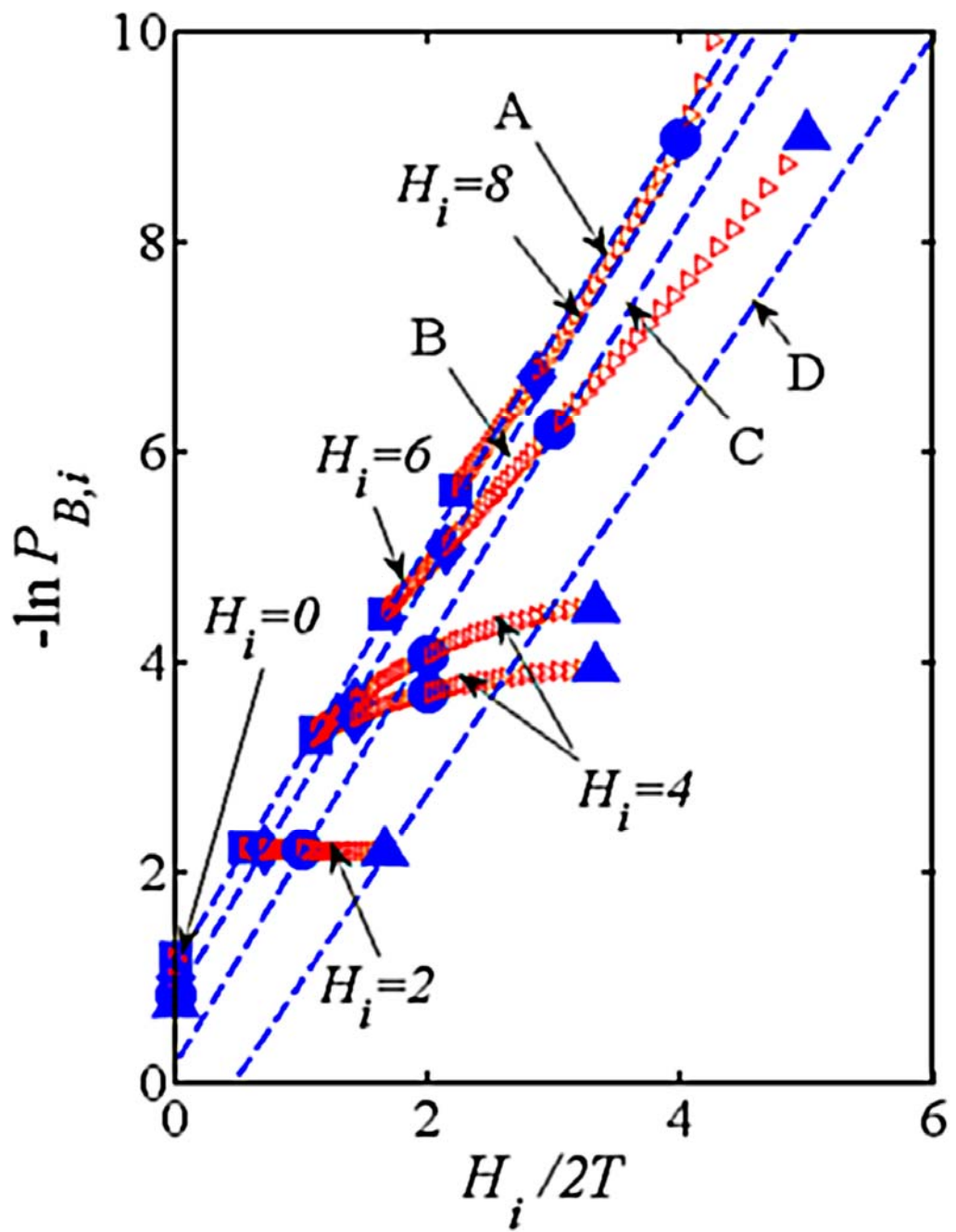


Fig.4 Xiao Xu et al.